ORIGINAL ARTICLE

Check for updates

Left ventricular concentric hypertrophy with cardiac magnetic resonance imaging improves risk stratification in patients with Duchenne muscular dystrophy: a prospective cohort study

Wei-feng Yuan[1,2] · Li Yu[3] · Ke Xu[1] · Rong Xu[1] · Hang Fu[1] · Yu Song[1] · Zi-qi Zhou[1] · Ting Xu[1] · Xiao-tang Cai[4] · Ying-kun Guo[1] · Hua-yan Xu[1]

Abstract

Background The development of left ventricular (LV) remodeling has been associated with an increased cardiovascular risk and cardiogenic death, and different patterns of remodeling result in varying levels of prognosis.

Objective To investigate the association between different patterns of LV remodeling and clinical outcomes in the preclinical stage of patients with Duchenne muscular dystrophy (DMD).

Materials and methods A total of 148 patients with DMD and 43 sex- and age-matched healthy participants were enrolled. We used the four-quadrant analysis method to investigate LV remodeling based on cardiac magnetic resonance (MR) imaging. Kaplan-Meier curves were generated to illustrate the event-free survival probability stratified by the LV remodeling pattern. Cox regression models were constructed and compared to evaluate the incremental predictive value of the LV remodeling pattern.

Results During the median follow-up period of 2.2 years, all-cause death, cardiomyopathy, and ventricular arrhythmia occurred in 5, 35, and 7 patients, respectively. LV concentric hypertrophy (hazard ratio 2.91, 95% confidence interval 1.47–5.75, P=0.002) was an independent predictor of composite endpoint events. Compared to the model without LV concentric hypertrophy, the model with LV concentric hypertrophy had significant incremental predictive value (chi-square value 33.5 vs. 25.2, P=0.004).

Conclusion Age and late gadolinium enhancement positivity were positively correlated with clinical outcomes according to the prediction models. LV concentric hypertrophy was also an independent predictor for risk stratification and provided incremental value for predicting clinical outcomes in the preclinical stage of patients with DMD.

Graphical Abstract
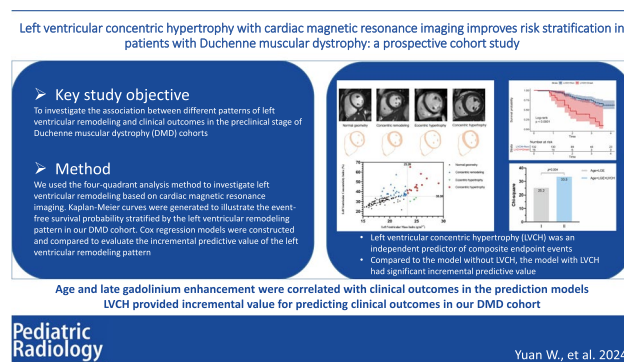
Wei-feng Yuan and Li Yu contributed equally to this work.

Extended author information available on the last page of the article

Introduction

Duchenne muscular dystrophy (DMD) is an X-linked recessive disease with an estimated worldwide incidence of approximately 1:3,500–6,300 live male births and a median life expectancy of 28.1 years [1, 2]. Heart failure is the cause of up to 40% of deaths in patients with DMD [3, 4]. The development of left ventricular (LV) remodeling has been related to increased cardiovascular risk and cardiogenic death [5–8]. Furthermore, LV remodeling has been observed in the mouse model of DMD [9]. Based on the four-quadrant analysis method, the morphology of the left ventricle can be divided into normal geometry and three types of remodeling (namely, concentric remodeling, eccentric hypertrophy, and concentric hypertrophy) [8, 10, 11]. However, the patterns of LV remodeling in patients with DMD are unclear. Importantly, different patterns of LV remodeling result in varying degrees of deleterious effects in the prognosis and clinical outcomes of cardiovascular diseases, particularly in the middle-aged and elderly population [8]. However, whether LV remodeling is associated with the occurrence of endpoint events in boys with DMD has not been established.

Cardiac magnetic resonance (MR) imaging is a noninvasive and non-ionizing radiation-based imaging modality for evaluating cardiac structure and function with excellent resolution [12]. Additionally, cardiac MR imaging has become an important standard for assessing LV remodeling [13]. As a conventional sequence in cardiac MR imaging, cine is easy to acquire and is a good imaging method for quantifying cardiac geometry, such as LV myocardial mass and end-diastolic volume, which are the basic parameters for defining LV remodeling [14, 15]. Therefore, we hypothesized that abnormal LV remodeling was detectable using cardiac MR imaging and might provide predictive value for risk stratification in the DMD cohort.

Materials and methods

Patient enrollment

This prospective study was conducted between September 2018 and December 2022. We obtained parental consent for all study participants before the examinations. The diagnosis of patients with DMD was based strictly on the diagnosis and management of DMD guidelines [16] and was confirmed by genetic testing, which identifies the presence of deletions, duplications, or mutations in the *dystrophin* gene. After obtaining approval from the ethics review board of the West China Second Hospital of Sichuan University (K2019056), we proceeded to advertise the recruitment and screened suitable healthy participants from the general population. The selected participants underwent a comprehensive assessment (without any history of cardiovascular disease or recent infection), were randomly assigned to the control group, and provided informed consent. A total of 215 patients with DMD were eligible, and 43 sex- and age-matched healthy participants were enrolled as controls. Due to refusal (written informed consent was not acquired from the enrolled subjects before the cardiac MR examination) or incomplete clinical data (missing rate was greater than 5%), 44 patients with DMD were excluded. The date of the first cardiac MR examination was recorded as the starting time. After the first cardiac MR acquisition, nine patients with DMD were excluded because of incomplete image data (any one sequence or parameter was missing based on the cardiac MR protocol below) or poor image quality (grade 1, according to a four-grade score for cardiac MR image quality below). During the follow-up period, eight patients were excluded because of loss to follow-up. The DMD patients included in this study underwent at least two cardiac MR examinations, as recommended by the guideline [17]. Finally, 148 patients who underwent cardiac MR examination at least twice were enrolled in the DMD group (Fig. 1). We defined the composite endpoint events as follows: all-cause death; cardiomyopathy with LV ejection fraction decline (an absolute LV ejection fraction ≤50% or a decline in LV ejection fraction ≥10% from the last cardiac MR study) [18, 19]; and ventricular arrhythmia (ventricular premature beat, ventricular tachycardia, ventricular flutter or ventricular fibrillation). When any of the above endpoint events was reached, the clinical outcome was considered to have occurred, and the onset date was recorded. If a patient had multiple endpoint events, the earliest onset event and its date were recorded. The DMD group was divided into the without-endpoint and with-endpoint groups.

Cardiac magnetic resonance protocol

All cardiac MR images were acquired on a 3-tesla whole-body MR scanner (MAGNETOM Skyra, Siemens Healthcare, Erlangen, Germany) with an 18-channel body phased-array coil during repeated breath-holds. For both the control and DMD groups, all sequences were acquired using breath-hold scanning. All participants were examined in the supine position. After localization of the heart, cine images were acquired using retrospective electrocardiogram-gated, balanced steady-state free precession pulse sequences including four-chamber long-axis slices and a stack of short-axis slices covering the whole heart. All the short-axis cine images were obtained with the following parameters: field of view (FOV)=300*241 mm^2; repetition time=3.42 ms; echo time=1.48 ms; flip angle=34°; slice thickness=6 mm; acquisition matrix=126×224; and 25 frames per cardiac cycle. Late gadolinium enhancement
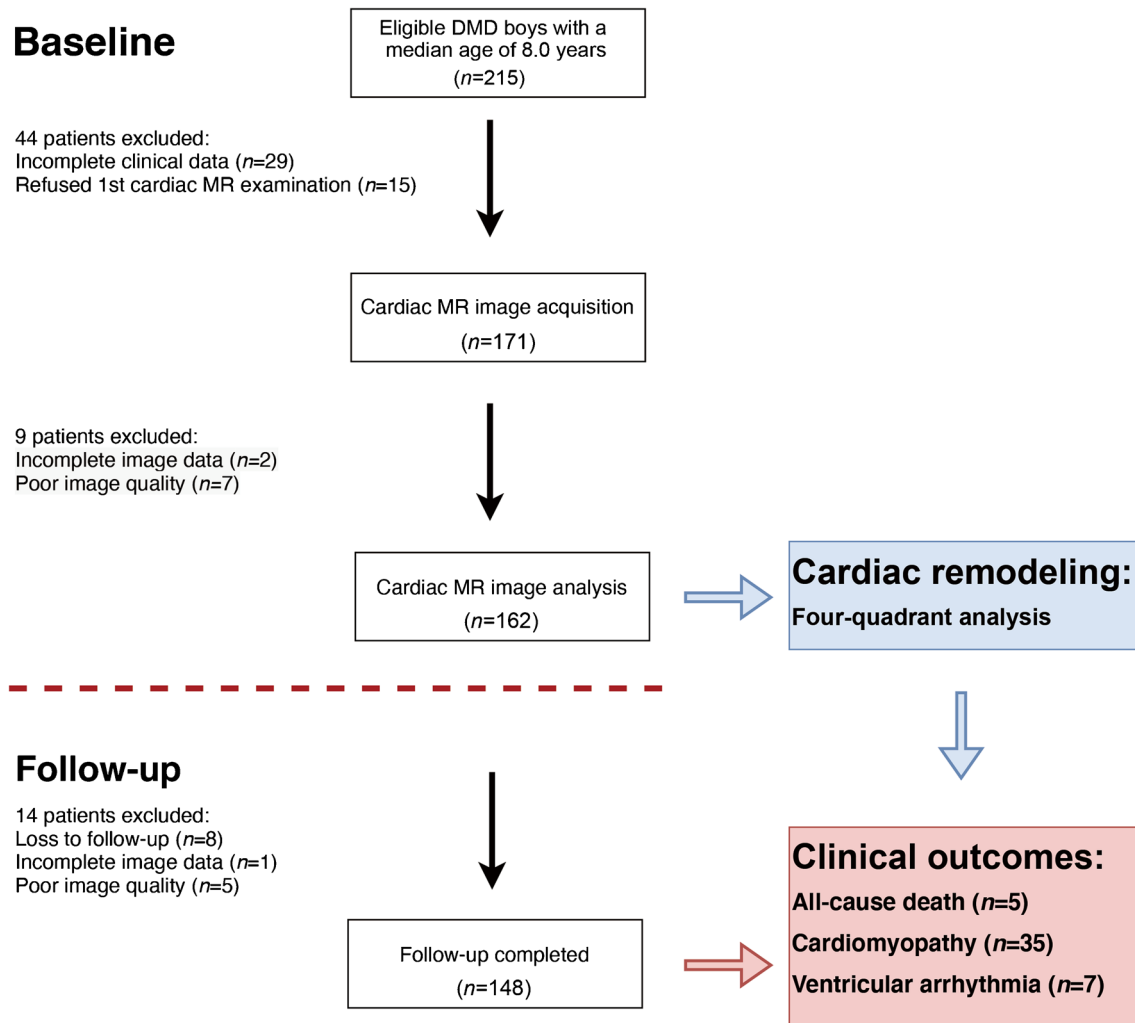
Baseline

Eligible DMD boys with a
median age of 8.0 years
(*n*=215)

44 patients excluded:
Incomplete clinical data (*n*=29)
Refused 1st cardiac MR examination (*n*=15)

Cardiac MR image acquisition
(*n*=171)

9 patients excluded:
Incomplete image data (*n*=2)
Poor image quality (*n*=7)

Cardiac MR image analysis
(*n*=162)

Cardiac remodeling:
Four-quadrant analysis

Follow-up

14 patients excluded:
Loss to follow-up (*n*=8)
Incomplete image data (*n*=1)
Poor image quality (*n*=5)

Follow-up completed
(*n*=148)

Clinical outcomes:
All-cause death (*n*=5)
Cardiomyopathy (*n*=35)
Ventricular arrhythmia (*n*=7)

Fig. 1 Flowchart of enrolled Duchenne muscular dysrtopy (DMD) patients in the prospective cohort study. *MR* magnetic resonance

images were acquired 5–10 min after intravenous injection at a dose of 0.1 mmol/kg gadolinium (Gadovist, Bayer Healthcare, Berlin, Germany). The corresponding parameters for late gadolinium enhancement were as follows: FOV=340*340 mm^2; repetition time=2.55 ms; echo time=1.09 ms; flip angle=55°; slice thickness=8 mm; and acquisition matrix=116×192. All participants in the control group underwent only one cardiac MR scan, specifically a cine sequence scan, without gadolinium contrast injection or late gadolinium enhancement scanning.

Magnetic resonance image post-processing and cardiac remodeling analysis

MR image analysis was carried out using the commercially available CVI42 software (Circle Cardiovascular Imaging Inc., Calgary, Canada). Cine images were first imported into the software. Then, the contours of the endocardium and epicardium were manually drawn at the end-diastolic phase in the short-axis and long-axis four-chamber images. LV end-diastolic volume, LV end-systolic volume, LV wall thickness, LV ejection fraction, and LV mass were computed automatically. LV mass was indexed to height$^{2.7}$, which has been shown to best predict cardiac risk compared to other methods of normalization [20]. LV concentricity index was defined as LV mass/LV end-diastolic volume [21, 22]. We used LV mass index to reflect the relative size of the overall LV morphology, and LV concentricity index to reflect the relative thickness of the overall LV wall. Cutoff values of LV mass index (23.28 g/m$^{2.7}$) and LV concentricity index (35.38%) based on the 95% reference range by percentile of healthy controls were used to classify all subjects into one of the four types based on the four-quadrant analysis method [8, 11]: normal geometry, LV concentric remodeling, LV eccentric hypertrophy, and LV concentric hypertrophy (Fig. 2).

The descriptions of the four types mentioned above are as follows:

a) Normal geometry: the overall wall thickness of the left ventricle is normal (normal LV concentricity index), and the overall morphology of the left ventricle is normal (normal LV mass index).
b) LV concentric remodeling: the overall wall thickness of the left ventricle becomes increased (increased LV concentricity index), but the overall morphology of the left ventricle is normal (normal LV mass index).
c) LV eccentric hypertrophy: the overall morphology of the left ventricle becomes larger (increased LV mass index), but the overall wall thickness of the left ventricle is normal (normal LV concentricity index).
d) LV concentric hypertrophy: the overall wall thickness of the left ventricle becomes increased (increased LV concentricity index), and the overall morphology of the left ventricle becomes larger (increased LV mass index).

The representative cardiac MR examples and diagrams of normal geometry and three LV remodeling types in DMD patients are shown in Fig. 2. The inter-observer reliability was estimated by comparing the measurements of the two radiologists (L.Y. with 5-year experience and H.X. with 6-year experience in cardiovascular imaging), who independently performed the calculations in a blinded manner. A four-grade score was used to assess the quality of cardiac MR images: extensive artifacts with poor image quality (grade 1); moderate artifacts not disturbing image analysis (grade 2); mild artifacts with good image quality (grade 3); and absence of artifacts with excellent image quality (grade 4). Only assessed images graded ≥ 2 were then included (see Supplementary Material 1 for examples).

Statistical analysis

Continuous variables are expressed as mean $\pm$ standard deviation for parametric variables or as median with interquartile range for nonparametric variables. The normality and variance homogeneity of the measurement data were analyzed using the Kolmogorov-Smirnov test and Levene test, respectively. Measurement data with normal distribution and homogeneity of variance were compared using one-way ANOVA. The non-normally distributed data were compared using the Mann-Whitney U test. The statistical significance of the differences

Fig. 2 **a** Cardiac magnetic resonance (MR) images and diagrams of normal geometry and three left ventricular (LV) remodeling types in Duchenne muscular dystrophy. **b** LV remodeling types were determined using previously defined cutoff values of LV mass index and LV concentricity index
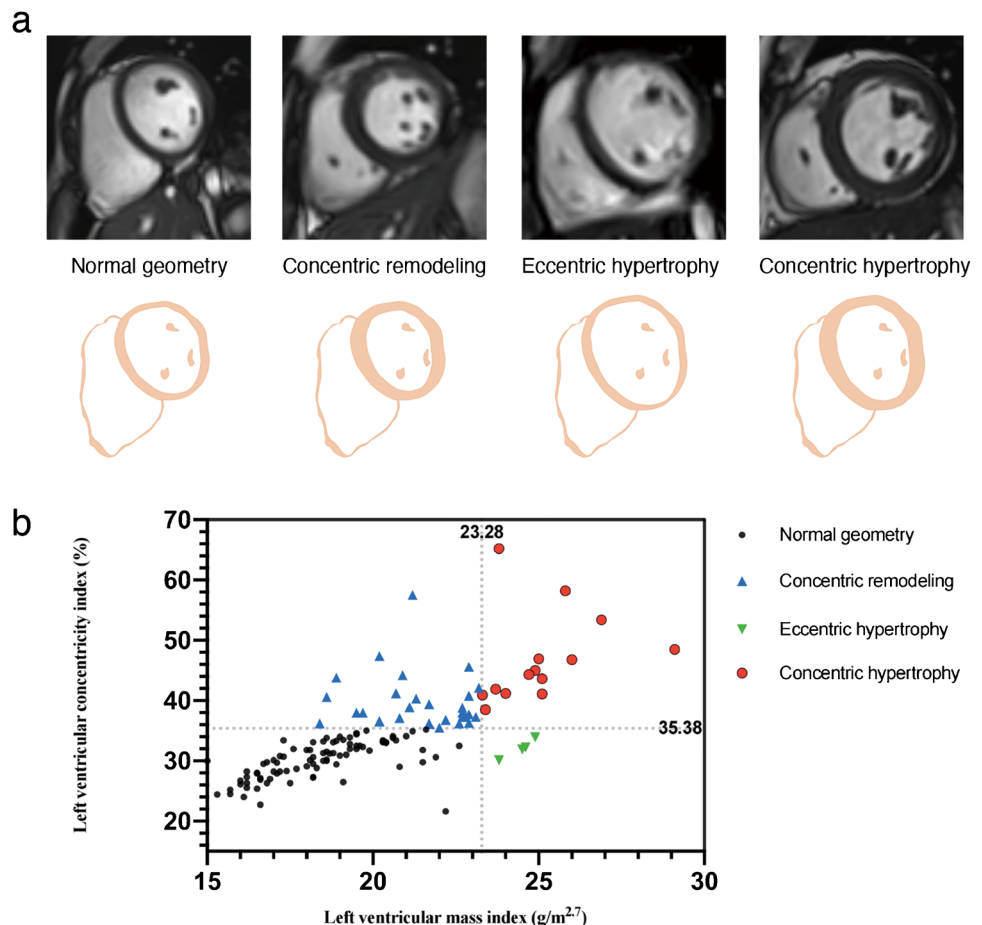
between enumeration data was assessed using the chi-square test or Fisher's exact probability method. Variables with *P* values <0.10 in the univariable analysis were candidates in multivariable analysis, using multivariable Cox proportional hazards regression analyses to determine the independent predictors of composite endpoint events. The cumulative incidences of composite endpoint events were presented as Kaplan-Meier estimates after comparison using the log-rank test. The likelihood ratio test was performed to calculate the incremental value between nested models, and the results are represented using chi-square value. Intra-observer and inter-observer reliabilities were evaluated using Bland-Altman analysis. A *P*<0.05 was considered statistically significant. Statistical Product and Service Solutions software version 26.0 (SPSS Inc., Chicago, IL), GraphPad Prism software (version 8.0, GraphPad Software, San Diego, CA), and R package version 3.5 (R Foundation for Statistical Computing, Vienna, Austria) were used for the statistical analyses.

Results

Clinical characteristics and outcomes

Clinical and imaging data were collected in 148 patients with DMD during a median follow-up of 2.2 years. During the follow-up period, 47 (31.8%) patients reached the composite endpoints. All-cause death occurred in five (10.6%) patients, whereas 35 (74.5%) patients experienced the onset of DMD-associated cardiomyopathy due to an absolute LV ejection fraction ≤50% or a decline in LV ejection fraction ≥10% from their last cardiac MR. In addition, ventricular arrhythmia occurred in seven (14.9%) patients in this study. Baseline characteristics and demographic data in controls, 101 (68.2%) patients without endpoint, and 47 (31.8%) patients with endpoint are illustrated in Table 1. Compared with the patients in the without-endpoint group, those in the with-endpoint group were older (median 9.7 vs. 8.0 years, *P*<0.001), had lower creatine kinase levels (median 11.1 vs. 12.8 U/mL, *P*=0.022), and had a greater frequency of late gadolinium enhancement positivity (65.3% vs. 40.8%, *P*=0.001). There were no significant differences in body fat percentage, body mass index, heart rate, blood pressure, glucocorticoid use, or cardiac medications between the subgroups.

Cardiac remodeling

The LV wall thickness (median 5.1 vs 4.7 mm, *P*=0.188) in the DMD group showed no significant difference compared with the healthy controls. Moreover, there was no significant difference in the LV wall thickness (median 5.3 vs 4.9 mm, *P*=0.436) between the with-endpoint group and the without-endpoint group. However, LV mass index (median 20.2 vs. 18.9 g/m$^{2.7}$, *P*=0.008) and LV concentricity index (median 34.6 vs 31.2, *P*<0.001) were significantly greater in the patients with endpoints than in those without. More than one-third of patients with DMD had three types of LV remodeling: 31 (20.9%) patients had LV concentric remodeling, four (2.7%) patients had LV eccentric hypertrophy, and 16 (10.8%) patients had LV concentric hypertrophy. Compared with the patients in the without-endpoint group, those in the with-endpoint group

Table 1 Demographic data of patients with and without endpoint in Duchenne muscular dystrophy

	Controls (*n*=43)	All patients (*n*=148)	Patients without endpoint (*n*=101)	Patients with endpoint (*n*=47)
Age, years	8.0 (7.0–9.0)	8.0 (7.0–9.8)	8.0 (7.0–9.0)	9.7 (7.9–11.0)[c]
Males, *n* (%)	43 (100.0)	148 (100.0)	101 (100.0)	47 (100.0)
Follow-up duration, years	–	2.2 (1.8–3.5)	2.5 (1.9–3.9)	1.9 (1.5–2.7)[c]
BMI, kg/m^2	16.7 (14.9–18.0)	17.5 (16.1–18.5)[a]	17.4 (16.0–18.5)	17.7 (16.3–18.5)
BFP, %	16.7 (14.3–19.5)	17.8 (16.0–20.4)[a]	17.5 (16.0–19.9)	19.4 (15.8–20.7)
Heart rate, bpm	99.0 (95.0–104.0)	101.5 (93.3–109.0)	102.0 (90.5–108.5)	100.0 (95.0–113.0)
SBP, mmHg	104.0 (94.0–109.0)	104.0 (100.0–110.0)	104.0 (99.5–107.5)	106.0 (101.0–111.0)
DBP, mmHg	64.0 (52.0–73.0)	64.0 (58.0–71.0)	64.0 (60.0–71.5)	65.0 (55.0–69.0)
Creatine kinase, U/mL	–	12.5 (10.1–15.6)	12.8 (10.6–16.6)	11.1 (8.9–15.1)[b]
LGE positivity, *n* (%)		70 (47.3)	35 (34.7)	35 (74.5)[c]
Glucocorticoids, *n* (%)		74 (50.0)	47 (46.5)	27 (57.4)
ACEI, *n* (%)		47 (31.8)	29 (28.7)	18 (38.3)
β-Blocker, *n* (%)		37 (25.0)	22 (21.8)	15 (31.9)
Coenzyme Q, *n* (%)		107 (72.3)	74 (73.3)	33 (70.0)

ACEI angiotensin converting enzyme inhibitor, *BFP* body fat percentage, *BMI* body mass index, *DBP* diastolic blood pressure, *DMD* Duchenne muscular dystrophy, *LGE* late gadolinium enhancement, *SBP* systolic blood pressure. [a]*P*<0.05 compared with controls; [b]*P*<0.05 and [c]*P*<0.001 compared with the patients without endpoint

had a lower probability of normal geometry (51.1% vs. 72.3%, $P=0.011$) and more frequent onset of LV concentric hypertrophy (25.5% vs. 4.0%, $P<0.001$) (Table 2). Intra-observer and inter-observer reliability for LV mass index was 0.89 (95% confidence interval [CI] 0.83–0.92) and 0.82 (95% CI 0.74–0.87), respectively. Intra-observer and inter-observer reliability for LV concentricity index was 0.96 (95% CI 0.95–0.98) and 0.89 (95% CI 0.85–0.93), respectively. In addition, the Bland-Altman plots for the intra-observer and inter-observer variability of the LV mass index and LV concentricity index are shown in Supplementary Material 2.

Survival analysis and risk stratification

In univariable analysis (Table 3), age (hazard ratio [HR] 1.31, 95% CI 1.16–1.48, $P<0.001$), late gadolinium enhancement positivity (HR 3.70, 95% CI 1.9–7.1, $P<0.001$), and LV concentric hypertrophy (HR 4.16, 95% CI 2.15–8.05, $P<0.001$) were associated with clinical outcomes. Kaplan-Meier curve illustrates the event-free survival probability stratified by the incidence of LV concentric hypertrophy. The subgroup with LV concentric hypertrophy had a lower probability of event-free survival compared to the subgroup without LV concentric hypertrophy in DMD patients (log-rank $P<0.001$, Fig. 3).

Incremental value analysis in Cox proportional-hazards models

Age, late gadolinium enhancement positivity, and LV concentric hypertrophy were subjected to multivariate analysis after undergoing multicollinearity testing. The two models

Table 3 Univariable analysis

	Composite endpoint		
	HR	95% CI	*P*-value
Age, years	1.31	1.16–1.48	<0.001
BMI, kg/m^2	1.01	0.92–1.11	0.773
BFP, %	1.03	0.97–1.09	0.342
Creatine kinase, U/mL	0.90	0.84–0.97	0.003
LGE positivity	3.70	1.9–7.1	<0.001
Glucocorticoids	1.24	0.69–2.20	0.475
ACEIs	1.23	0.68–2.21	0.500
β-Blockers	1.38	0.75–2.56	0.299
Coenzyme Q	0.73	0.39–1.38	0.334
LVEDVI (mL/m^2)	0.94	0.91–0.97	<0.001
LVESVI (mL/m^2)	1.06	1.00–1.11	0.031
LVMI (g/m^2)	1.12	1.03–1.21	0.011
LVCI (%)	1.04	1.02–1.06	<0.001
LVCR	1.03	0.51–2.08	0.926
LVEH	0.97	0.13–7.07	0.977
LVCH	4.16	2.15–8.05	<0.001

ACEIs angiotensin converting enzyme inhibitors, *BFP* body fat percentage, *BMI* body mass index, *CI* confidence interval, *HR* hazard ratio, *LGE* late gadolinium enhancement, *LVCH* left ventricular concentric hypertrophy, *LVCI* left ventricular concentricity index, *LVCR* left ventricular concentric remodeling, *LVEDVI* left ventricular end-systolic volume indexed to body surface area, *LVEH* left ventricular eccentric hypertrophy, *LVESVI* left ventricular end-diastolic volume indexed to body surface area, *LVMI* left ventricular myocardial mass indexed to body surface area

were subsequently established to evaluate the incremental predictive value of LV concentric hypertrophy using Cox proportional-hazards regression analysis. The basic model

Table 2 Comparison of the quantitative parameters of left ventricular remodeling in Duchenne muscular dystrophy

	Controls (*n*=43)	All patients (*n*=148)	Patients without endpoint (*n*=101)	Patients with endpoint (*n*=47)
LV geometry parameters				
LVWT, mm	4.7 (3.8–5.8)	5.1 (4.1–6.1)	4.9 (4.1–6.0)	5.3 (4.1–6.2)
LVMI, g/m$^{2.7}$	18.2 (16.5–19.2)	19.3 (17.3–21.7)[a]	18.9 (17.0–21.4)	20.2 (18.2–23.7)[b]
LVCI, %	28.1 (24.0–31.3)	32.5 (28.7–37.0)[a]	31.2 (27.9–35.4)	34.6 (32.0–43.6)[c]
LVEDVI, mL/m^2	62.9 (56.9–68.4)	60.4 (56.4–61.9)[d]	61.2 (60.0–62.6)	56.1 (55.0–56.9)[c]
LVESVI, mL/m^2	22.8 (17.1–27.0)	23.3 (18.9–27.7)	23.1 (18.9–26.5)	26.2 (19.3–31.1)[b]
LV remodeling types				
Normal geometry, *n* (%)	–	97 (65.5)	73 (72.3)	24 (51.1)[c]
LVCR, *n* (%)		31 (20.9)	21 (20.8)	10 (21.3)
LVEH, *n* (%)		4 (2.7)	3 (3.0)	1 (2.1)
LVCH, *n* (%)		16 (10.8)	4 (4.0)	12 (25.5)[d]

LV left ventricular, *LVCH* left ventricular concentric hypertrophy, *LVCI* left ventricular concentricity index, *LVCR* left ventricular concentric remodeling, *LVEDVI* left ventricular end-systolic volume indexed to body surface area, *LVEH* left ventricular eccentric hypertrophy, *LVESVI* left ventricular end-diastolic volume indexed to body surface area, *LVMI* left ventricular myocardial mass indexed to height$^{2.7}$, *LVWT* left ventricular wall thickness. [a]$P<0.01$ and [d]$P<0.05$ compared with controls; [b]$P<0.05$ and [c]$P<0.001$ compared with the patients without endpoint

included age and late gadolinium enhancement positivity as independent predictors of composite endpoint events in DMD patients. The new model incorporated the addition of LV concentric hypertrophy compared to the basic model (Table 4). The method was performed for calculating the incremental value between nested models [23]. Compared to the basic model, the new model had significant incremental predictive value (chi-square value 33.5 vs. 25.2, *P*=0.004), as illustrated in Fig. 4.

Discussion

In this DMD study, 97 patients exhibited normal geometry, while 51 had onset of three types of LV remodeling at baseline. During a median follow-up of 2.2 years, 47 patients reached the composite endpoints. Age and late gadolinium enhancement positivity were positively correlated with clinical outcomes according to the prediction models. As a pattern of LV remodeling, LV concentric hypertrophy emerged as an independent predictor of event-free survival in DMD patients, offering incremental value for risk stratification.

Among the DMD patients with composite endpoint events, nearly three-quarters experienced the onset of DMD-associated cardiomyopathy (LV ejection fraction decline) in our study. The onset of cardiac dysfunction may occur more frequently than all-cause death and ventricular arrhythmia in the "early-stage" DMD patients. A previous study revealed that "late-stage" DMD patients have abnormal LV wall thickness at end-systole and a poor prognosis [24]. However, we found that LV wall thickness not only failed to predict the occurrence of cardiac-related endpoint events in DMD patients, but

Table 4 Multivariable proportional-hazard models

	Composite endpoint		
	HR	95% CI	*P*-value
Model I			
Age, years	1.20	1.05–1.37	0.009
LGE positivity	2.57	1.25–5.29	0.01
Model II			
Age, years	1.20	1.04–1.38	0.014
LGE positivity	2.16	1.02–4.58	0.044
LVCH	2.91	1.47–5.75	0.002

CI confidence interval, *HR* hazard ratio, *LGE* late gadolinium enhancement, *LVCH* left ventricular concentric hypertrophy

also barely distinguished the differences in myocardial morphology between DMD patients and the healthy participants in this study. Thus, cardiac remodeling evaluated by LV wall thickness might be inconspicuous in "early-stage" patients with DMD. It was essential to select and process cardiac geometric data from different dimensions to evaluate the patterns of cardiac remodeling and its relationship to clinical outcomes in the "early-stage" DMD. As the fundamental indicators for evaluating cardiac remodeling, LV mass index (overall morphology) and LV concentricity index (overall wall thickness) were significantly associated with composite endpoint events in the univariable analysis. Interestingly, the multivariable analysis showed that neither LV mass index nor LV concentricity index, but LV concentric hypertrophy was an independent predictor of event-free survival possibility in patients with DMD. When LV mass index and LV concentricity index were greater than 23.28 g/m$^{2.7}$ and 35.38% respectively in a

Fig. 3 Kaplan-Meier curves illustrate the event-free survival probability stratified by left ventricular concentric hypertrophy (LVCH). The onset-LVCH subgroup had a lower probability of event-free survival compared to the non-LVCH subgroup
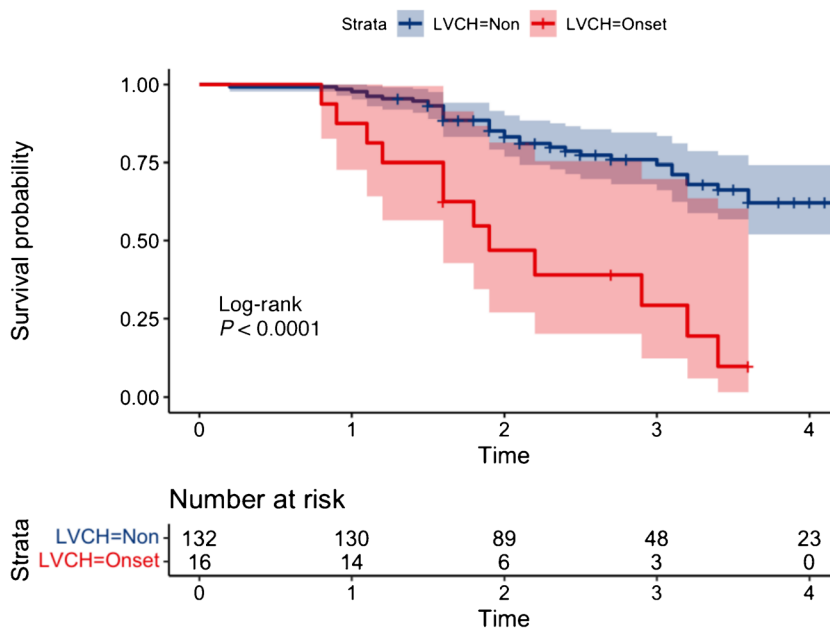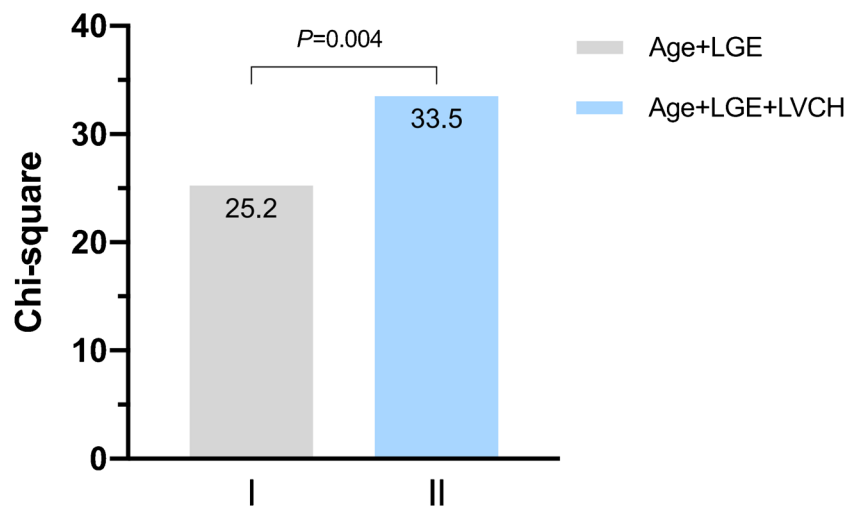
Fig. 4 Incremental predictive value of left ventricular concentric hypertropy (LVCH) according to the Cox regression model. Compared to the model without LVCH, the model with LVCH had significant incremental predictive value. *LGE* late gadolinium enhancement

DMD patient, we considered that LV concentric hypertrophy occurred. Our main conjecture was that LV concentric hypertrophy reflected the changes in both the overall wall thickness and the overall morphology. The clinical phenomenon might indirectly validate the conclusions regarding the underlying mechanisms from the previous animal experiment [9]. Previous studies have also confirmed that cardiomyocyte hypertrophy has already occurred in patients with "early-stage" DMD [3, 25]. The onset of LV concentric hypertrophy in our study also supported the above mechanism. In addition, it has been reported that some children with obesity experience the onset of LV concentric hypertrophy [10]. Obesity is relatively common in patients with DMD due to the fat replacement and the side effects caused by glucocorticoids [26, 27]. In clinical practice, it might be crucial to monitor the occurrence of LV concentric hypertrophy in patients with DMD and maintain a vigilant approach toward the development of various adverse cardiac prognoses.

As expected, age and late gadolinium enhancement were independent predictive factors for composite endpoint events, consistent with previous studies assessing clinical outcomes in boys with DMD [24]. Undoubtedly, age serves as a reliable indicator of the overall disease progression in patients with DMD. A previous study has shown a strong correlation between creatine kinase and the motor function of patients with DMD, indicating that creatine kinase may also reflect the overall disease progression to some extent. However, creatine kinase did not enter the multivariate analysis after undergoing tests for multicollinearity in our study. Similarly, unexpected, as an indicator reflecting the overall degree of obesity, body mass index did not demonstrate predictive value for composite endpoint events in this study. We speculated that these findings might be related to the overall baseline levels of the enrolled patients being in the early stage of the disease progression. In addition, Menon et al. reported that late gadolinium enhancement positivity, a marker of myocardial fibrosis,

could be applied as a screening tool to detect patients at risk for cardiac-related outcomes in DMD cohort [28]. Thus, the ability of late gadolinium enhancement positivity to independently predict the occurrence of cardiovascular endpoint events was convincing in our study. Due to the cautious use requirement of gadolinium contrast agents, we carefully controlled the dose at 0.1 mmol/kg in this study. Therefore, we set the optimal image acquisition time to "5–10 min" to ensure that the gadolinium contrast agent was captured before clearance. If subsequent researchers use a gadolinium contrast agent dose greater than 0.1 mmol/kg, we recommend extending the optimal image acquisition time appropriately to obtain the best late gadolinium enhancement images. Rudolph et al. discovered a significant correlation between myocardial fibrosis, as indicated by late gadolinium enhancement, and myocardial mass [14]. Myocardial fibrosis may serve as one of the histopathological foundations for cardiac remodeling and LV hypertrophy in cardiomyopathies. However, late gadolinium enhancement is not sufficient to reflect LV hypertrophy solely based on the cardiac morphological structure. Although we acknowledge the advantages of echocardiography in assessing changes in cardiac morphology, currently it seems that echocardiography is temporarily unable to match late gadolinium enhancement in evaluating myocardial fibrosis, making it difficult to achieve a comprehensive evaluation of LV remodeling in DMD patients in a "one-stop" manner. Cardiac magnetic resonance holds the promise of providing a one-stop, efficient evaluation of LV remodeling by simultaneously assessing cardiac morphology and histopathology in DMD patients. Building upon the basic model constructed using age (reflecting overall disease progression) and late gadolinium enhancement positivity (reflecting cardiac histopathological progression), LV concentric hypertrophy (reflecting cardiac morphological progression) showed significant incremental predictive value. It is worth emphasizing that the likelihood ratio test based on nested models is the only test required to evaluate whether new predictor variables should

be added to the existing model, and calculating the area under the curve or concordance index is not recommended [23, 29, 30]. Thus, we performed the likelihood ratio test and calculated the chi-square values for evaluating the incremental predictive value of LV concentric hypertrophy. The results indicate that LV concentric hypertrophy could be regarded as a valuable tool for detecting subtle remodeling of left ventricle, thereby facilitating a more precise prediction of clinical outcomes in patients with early-stage DMD. Even for initially LV concentric hypertrophy-negative patients, we believe that monitoring the occurrence of LV concentric hypertrophy during follow-up examinations is necessary to remain vigilant about the occurrence of adverse clinical outcomes in DMD patients.

There are several limitations of our study. First, we did not consider the cumulative dose of glucocorticoids or cardiac medications. Second, we did not analyze left atrial or right ventricular remodeling parameters, which might interact with left ventricle remodeling in DMD patients. Finally, the predictive effectiveness of LV concentric hypertrophy for the clinical outcomes in DMD was not externally validated.

Conclusion

In this study, we found that LV concentric hypertrophy emerged as an independent predictor for risk stratification and provided incremental value for predicting clinical outcomes in the early-stage DMD cohort. Additionally, we established cutoff values for cardiac MR images to help diagnose LV concentric hypertrophy and evaluate inconspicuous remodeling in DMD patients.

Declarations

References

1. Landfeldt E, Thompson R, Sejersen T et al (2020) Life expectancy at birth in Duchenne muscular dystrophy: a systematic review and meta-analysis. Eur J Epidemiol 35:643–653
2. Broomfield J, Hill M, Guglieri M et al (2021) Life expectancy in Duchenne muscular dystrophy: reproduced individual patient data meta-analysis. Neurology 97:e2304–e2314
3. D'Amario D, Amodeo A, Adorisio R et al (2017) A current approach to heart failure in Duchenne muscular dystrophy. Heart 103:1770–1779
4. Jefferies JL, Eidem BW, Belmont JW et al (2005) Genetic predictors and remodeling of dilated cardiomyopathy in muscular dystrophy. Circulation 112:2799–2804
5. Lieb W, Gona P, Larson MG et al (2014) The natural history of left ventricular geometry in the community: clinical correlates and prognostic significance of change in LV geometric pattern. JACC Cardiovasc Imaging 7:870–878
6. Lu C, Chen J, Suksaranjit P et al (2020) Regional myocardial remodeling characteristics correlates with cardiac events in sarcoidosis. J Magn Reson Imaging 52:499–509
7. Rodriguez-Palomares JF, Gavara J, Ferreira-González I et al (2019) Prognostic value of initial left ventricular remodeling in patients with reperfused STEMI. Jacc-cardiovasc Imag 12:2445–2456
8. Krumholz HM, Larson M, Levy D (1995) Prognosis of left ventricular geometric patterns in the Framingham heart study. J Am Coll Cardiol 25:879–884
9. Greally E, Davison BJ, Blain A et al (2013) Heterogeneous abnormalities of in-vivo left ventricular calcium influx and function in mouse models of muscular dystrophy cardiomyopathy. J Cardiovasc Magn Reson 15:4
10. Jing L, Binkley CM, Suever JD et al (2016) Cardiac remodeling and dysfunction in childhood obesity: a cardiovascular magnetic resonance study. J Cardiovasc Magn Reson 18:28
11. Ganau A, Devereux RB, Roman MJ et al (1992) Patterns of left ventricular hypertrophy and geometric remodeling in essential hypertension. J Am Coll Cardiol 19:1550–1558
12. Ng ACT, Delgado V, Borlaug BA, Bax JJ (2021) Diabesity: The combined burden of obesity and diabetes on heart disease and the role of imaging. Nat Rev Cardiol 18:291–304
13. Pezel T, Viallon M, Croisille P et al (2021) Imaging interstitial fibrosis, left ventricular remodeling, and function in stage A and B heart failure. JACC Cardiovasc Imaging 14:1038–1052
14. Rudolph A, Abdel-Aty H, Bohl S et al (2009) Noninvasive detection of fibrosis applying contrast-enhanced cardiac magnetic resonance in different forms of left ventricular hypertrophy relation to remodeling. J Am Coll Cardiol 53:284–291
15. Jing L, Nevius CD, Friday CM et al (2017) Ambulatory systolic blood pressure and obesity are independently associated with left ventricular hypertrophic remodeling in children. J Cardiovasc Magn Reson 19:86
16. Bushby K, Finkel R, Birnkrant DJ et al (2010) Diagnosis and management of Duchenne muscular dystrophy, part 1: diagnosis, and pharmacological and psychosocial management. Lancet Neurol 9:77–93
17. Birnkrant DJ, Bushby K, Bann CM et al (2018) Diagnosis and management of Duchenne muscular dystrophy, part 2: respiratory, cardiac, bone health, and orthopaedic management. Lancet Neurol 17:347–361
18. Feingold B, Mahle WT, Auerbach S et al (2017) Management of cardiac involvement associated with neuromuscular diseases: a scientific statement from the American Heart Association. Circulation 136:e200–e231
19. Siddiqui S, Alsaied T, Henson SE et al (2020) Left ventricular magnetic resonance imaging strain predicts the onset of Duchenne

muscular dystrophy-associated cardiomyopathy. Circ Cardiovasc Imaging 13:e011526

20. de Simone G, Daniels SR, Devereux RB et al (1992) Left ventricular mass and body size in normotensive children and adults: assessment of allometric relations and impact of overweight. J Am Coll Cardiol 20:1251–1260

21. Xu L, Keenan BT, Maislin D et al (2021) Effect of obstructive sleep apnea and positive airway pressure therapy on cardiac remodeling as assessed by cardiac biomarker and magnetic resonance imaging in nonobese and obese adults. Hypertension 77:980–992

22. Amier RP, Marcks N, Hooghiemstra AM et al (2021) Hypertensive exposure markers by MRI in relation to cerebral small vessel disease and cognitive impairment. JACC Cardiovasc Imaging 14:176–185

23. Vickers AJ, Cronin AM, Begg CB (2011) One statistical test is sufficient for assessing new predictive markers. BMC Med Res Methodol 11:1–7

24. Cha JJ, Kim IS, Kim JY et al (2022) The association between cardiac involvement and long-term clinical outcomes in patients with Duchenne muscular dystrophy. ESC Heart Fail 9:2199–2206

25. D'Amario D, Gowran A, Canonico F et al (2018) Dystrophin cardiomyopathies: clinical management, molecular pathogenesis and evolution towards precision medicine. J Clin Med 7:291

26. Birnkrant DJ, Bushby K, Bann CM et al (2018) Diagnosis and management of Duchenne muscular dystrophy, part 1: diagnosis, and neuromuscular, rehabilitation, endocrine, and gastrointestinal and nutritional management. Lancet Neurol 17:251–267

27. Henson SE, Lang SM, Khoury PR et al (2021) The effect of adiposity on cardiovascular function and myocardial fibrosis in patients with Duchenne muscular dystrophy. J Am Heart Assoc 10:e021037

28. Menon SC, Etheridge SP, Liesemer KN et al (2014) Predictive value of myocardial delayed enhancement in Duchenne muscular dystrophy. Pediatric Cardiol 35:1279–1285

29. Cook NR (2018) Quantifying the added value of new biomarkers: how and how not. Diagn Progn Res 2:14

30. Moons KG, de Groot JA, Linnet K et al (2012) Quantifying the added value of a diagnostic test or marker. Clin Chem 58:1408–1417

Authors and Affiliations

Wei-feng Yuan[1,2] **· Li Yu**[3] **· Ke Xu**[1] **· Rong Xu**[1] **· Hang Fu**[1] **· Yu Song**[1] **· Zi-qi Zhou**[1] **· Ting Xu**[1] **· Xiao-tang Cai**[4] **· Ying-kun Guo**[1] **· Hua-yan Xu**[1]

✉ Hua-yan Xu
xuhuayan2022.09_@scu.edu.cn

1 Department of Radiology, Key Laboratory of Birth Defects and Related Diseases of Women and Children of Ministry of Education, West China Second University Hospital, Sichuan University, 20# Section 3 South Renmin Road, Chengdu 610041, China

2 Department of Medical Imaging, Clinical Medical College and The First Affiliated Hospital of Chengdu Medical College, Chengdu, China

3 Department of Pediatric Cardiovascular Medicine, West China Second University Hospital, Sichuan University, Chengdu, China

4 Department of Rehabilitation, Key Laboratory of Birth Defects and Related Diseases of Women and Children of Ministry of Education, West China Second University Hospital, Sichuan University, Chengdu, China